Electronic Supplementary Material (ESI) for ChemComm.

SUPPORTING INFORMATION

A robust and unique iron(II) Mosaic-like MOF architecture

Estefania Fernandez-Bartolome[a], José Santos[a], Saeed Khodabakhshi[a], Laura J. McCormick[b], Simon J. Teat[b], Cristina Saenz de Pipaon[c], Jose R. Galan-Mascarós[c], Nazario Martín[a,d], Jose Sanchez Costa*[a]

[a] IMDEA Nanociencia, C/ Faraday 9, Ciudad Universitaria de Cantoblanco, 28049, Madrid, Spain.
[b] Advanced Light Source, Berkeley Laboratory, 1; Cyclotron Road, CA 94720, Berkeley, US.
[c] ICIQ, Avda. Països Catalans, 16; 43007, Tarragona, Spain.
[d] Facultad de Ciencias Químicas, Universidad Complutense de Madrid, Madrid, 28040, Spain

1) Experimental Section

Materials. Chemicals and reagents were purchased from commercial suppliers and used as received.

Physical measurements.

- NMR spectra were recorded on a Bruker Advance 300 (1H: 400 MHz) spectrometer at 298 K using partially deuterated solvents as internal standards. Coupling constants (J) are denoted in Hz and chemical shifts (δ) in ppm. Multiplicities are denoted as follows: s = singlet, d = doublet, t = triplet, m = multiplet.
- FT-IR spectra were recorded as neat samples in the range 400-4000 cm-1on a Bruker Tensor 27 (ATR device) Spectrometer.
- TGA was performed using a TA Instrument TGAQ500 with a ramp of 2 ºC/min under air and nitrogen from 30 to 500 ºC.
- Elemental analyses (C, H and N) were performed on a LECO CHNS-932 Analyzer at the "Servicio Interdepartamental de Investigación (SIdI)" at Autónoma University of Madrid.
- Gas isotherm measurement was carried out on a Micromeritics Flowsorb 2300 and it was performed at 77 K, with the temperature held constant using liquid N_2 bath.
- Crystal Structure Determination: The data were collected with an orange block crystal of 1 with a Bruker APEX II CCD diffractometer at the Advanced Light Source beamline 11.3.1 at Lawrence Berkeley National Laboratory from a silicon (111) mono- chromator (T = 100, K, λ = 0.7749 Å). The crystal was taken directly from its solution, mounted with a drop of Paratone-N oil and immediately put into the cold stream of dry N_2 on the goniometer. The structure was solved by direct methods and the refinement on F^2 and all further calculations were carried out with the SHELX-TL suite.[61]
- Powder X-ray diffratograms were obtained by using a Panalytical X'Pert PRO diffractometer (Cu-Kα1 X-radiation, λ1=1.5406 Å) with parallel-beam collimator, graphite secondary monochromator and Xenon detector. Theta / 2 theta sweep has been carried out from 5º to 90º range with an angular increase of 0,04º. Diffraction patterns were recorded at room temperature.
- Magnetic susceptibility measurements between 2-300 K were carried out in a Quantum Design MPMS-XL SQUID magnetometer under a 1000 Oe field. Each sample was secured inside a gel capsule with glass wool, and the capsule was pinched (0.5 mm diameter hole) on the top to allow convenient purging of the interior of the capsule. Pascal constants were used to correct for the diamagnetic contribution.

2) Synthesis of the PM-Tria Ligand (*N*,*N*′E,*N*,*N*′E)-*N*,*N*′-(1,4-phenylenebis(methanylylidene))bis(4*H*-1,2,4-3)

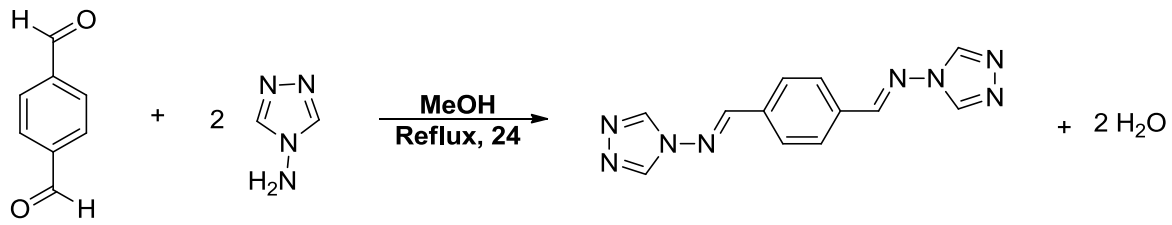

A mixture of terephthalaldehyde (0.670 g, 5 mmol) and 4-amino-1,2,4-triazole (1.680 g, 20 mmol) in methanol (30 mL) was refluxed until completion was observed by TLC (hexane/EtOAc 2:1) after 24 h. Upon cooling to room temperature, the resulting off-white precipitate was filtered off and thoroughly washed with methanol. Further purification was achieved by recrystallisation from DMSO, yielding a bright white solid (1.318 g, 95%). ^{1}H NMR (400 MHz, DMSO-d$_6$, δ): 9.18 (s, 4H, benzyl ring), 9.17 (s, 2H, N=CH–Ar), 8.03 (s, 4H, triazole ring) ppm. FTIR (neat): 3126, 3081, 1683, 1608, 1514, 1493, 1463, 1316, 1287, 1213, 1165, 1053, 831, 721, 619, 536, 489 cm^{-1}. (See Figure S1)

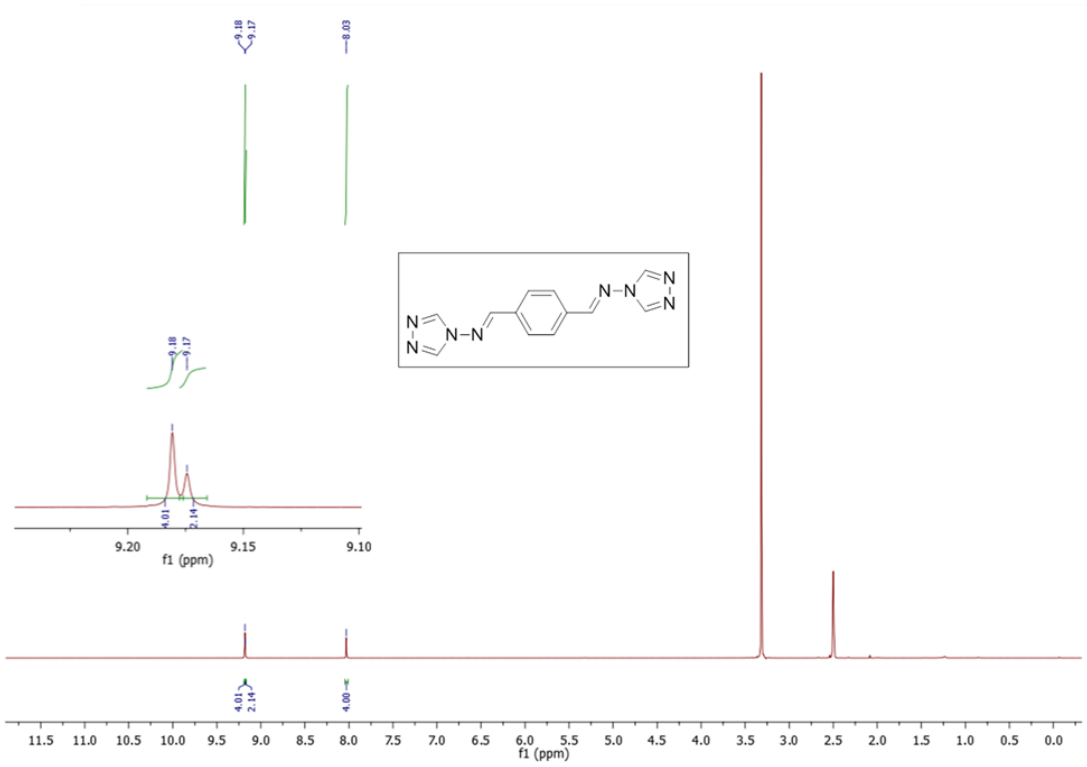

Figure S1. ^{1}H NMR (400 MHz, DMSO-d^6, 298 K) of the **PM-Tria**.

3) Synthesis of $\{[Fe(L)_2(\mu\text{-}F)](BF_4)\}_n$ (1)

i) A suspension of iron(II) tetrafluoroborate hexahydrate (19 mg, 0.056 mmol) and ascorbic acid (approx. 3 mg) in ethanol (4 mL) was added to a suspension of **PM-Tria,** (20 mg, 0.075 mmol) in ethanol (8 mL) and stirred for 10 minutes giving a cloudy solution. The mixture was transferred into a Parr reactor, sealed, and kept at 140 °C for 4 days in a furnace and cooled to room temperature. Small red crystals suitable for X-ray diffraction were formed after 4 days (20%, 3.9 mg)

ii) A suspension of iron(II) tetrafluoroborate hexahydrate (9.3 mg, 0.028 mmol), iron(II) fluoride (2.62 mg, 0.028 mmol) and ascorbic acid (approx. 3 mg) in ethanol (4 mL) was added to **PM-Tria**, (20 mg, 0.075 mmol) in ethanol (8 mL) and stirred for 10 minutes giving a cloudy solution. The mixture was transferred into a Parr reactor, sealed, and warmed at 140 °C for 4 days in a furnace and cooled to room temperature. Small red crystals suitable for X-ray diffraction were formed (38.60%, 7.5 mg).

IR: 3565(w), 3118 (w), 1617 (w), 1506 (m), 1403 (w), 1325 (w), 1295 (w), 1212 (m), 1167 (m), 1061 (s) this band is assigned to the B-F vibration of the $BF4^-$ counter ion (Figure S3), 969 (s), 872 (m), 833 (m), 733 (m), 719 (m), 675 (w), 625 (s), 538 (m), 536 (m), 493 (s), 454 (s), 443 (s), 430 (s) the last three peaks correspond to the Fe-F vibration (Figure S4); elemental analysis calculated (%) for $C_{24}H_{20}N_{16}FeF_5B.0.5\ C_2H_6O.\ 1.7\ H_2O(\{[Fe(L)_2(\mu\text{-}F)](BF_4)\}_n.0.5.\ C_2H_6O.\ 1.7\ H_2O$): C 40.15, N 29.97, H 3.56; found C 40.15, N 29.99, H 3.54.

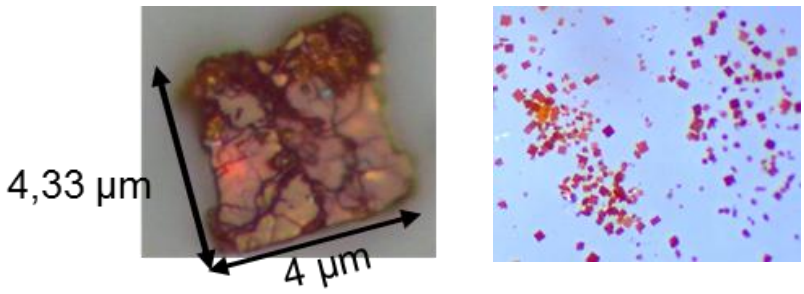

Figure S2. View of a single crystal obtained directly from the synthesis of 1 and a global view of different sample 1 showing the homogeneity of the crystalline size.

4) Infrared Spectra of iron(II) salts, PM-Tria ligand and compound(1)

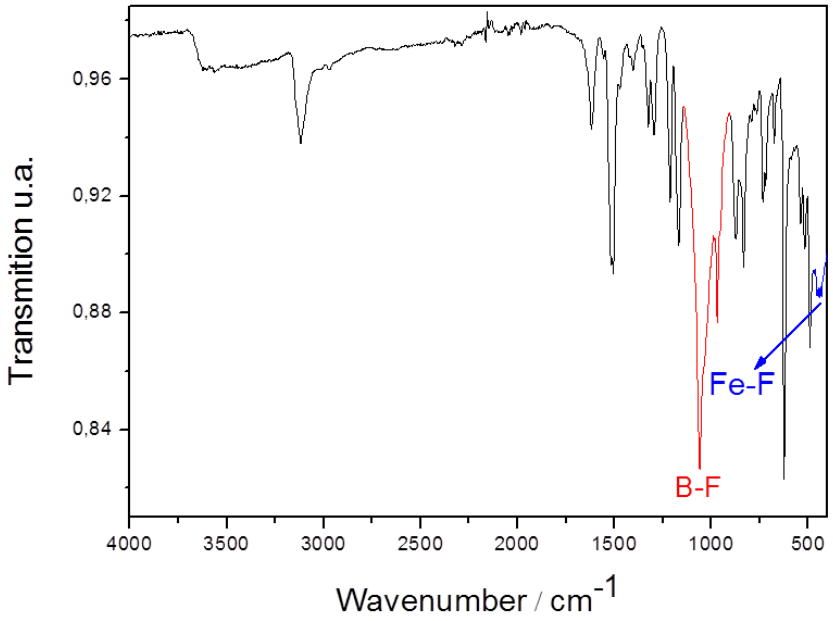

Figure S3. Infrared Spectrum of compound (1)

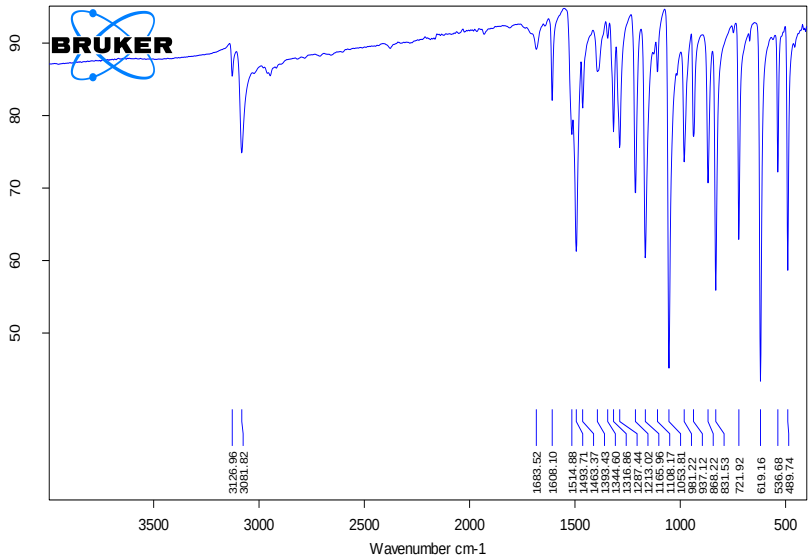

Figure S4. Infrared spectrum of ligand PM-Tria

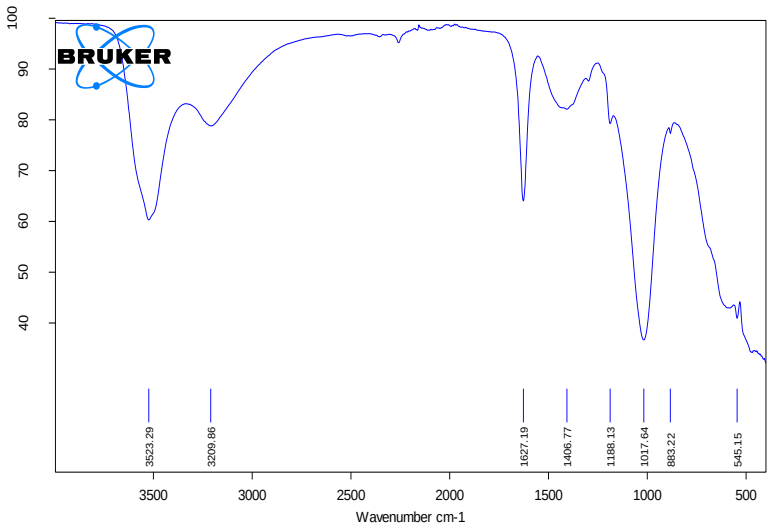

Figure S5. Infrared Spectrum of $Fe(BF_4)_2$

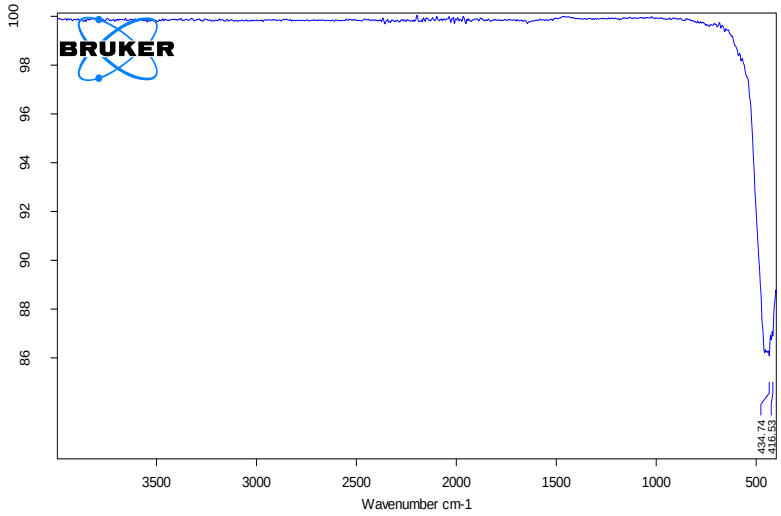

Figure S6. Infrared Spectrum of FeF_2

5) Thermogravimetric analysis of compound 1

Thermogravimetric profile of **1** (0.2670 mg in air (Figure S7) showing the mass variation (green curve) and its first derivative (blue curve) upon heating at 2 ºC/min. In the thermogravimetric analysis (Figure S7), the material presents a high thermal stability, starting to decompose at temperatures above 225 ºC which implies high robustness

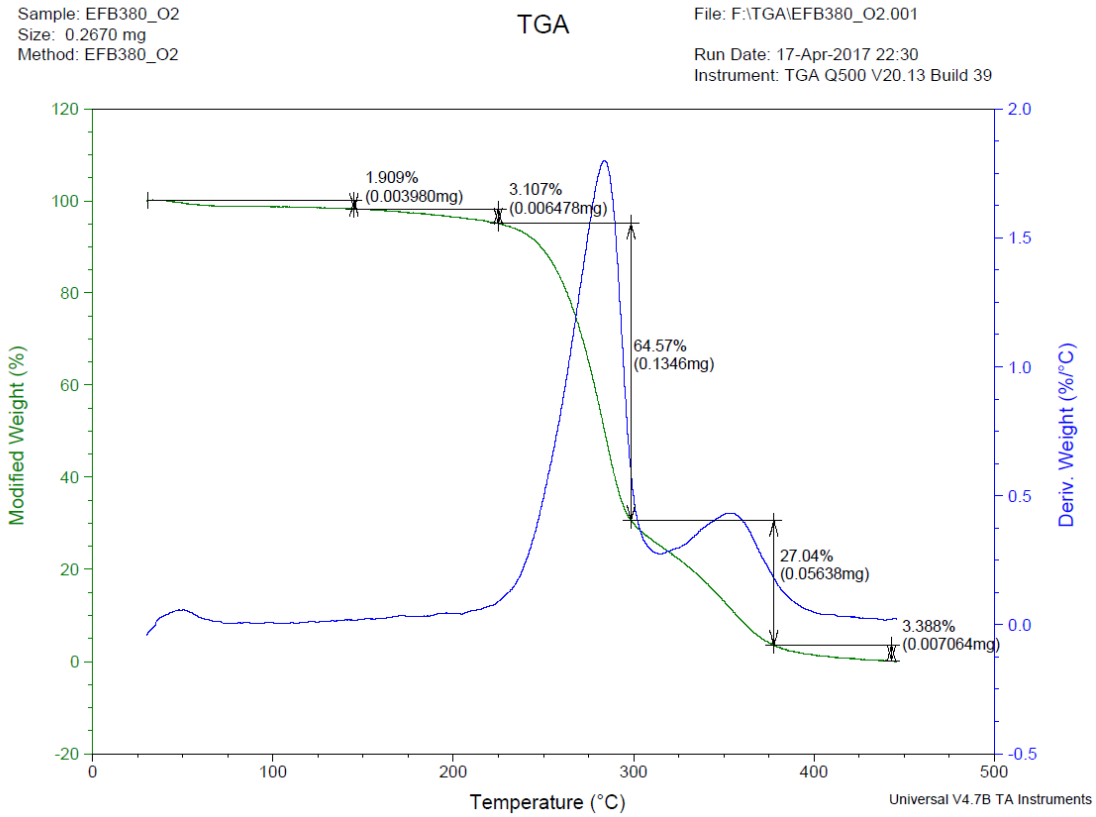

Figure S7.Thermogravimetric analysis of **1** run in air at a heating rate of 2ºC min^{-1}

6) X-ray Powder Diffraction (XRD) of compound 1

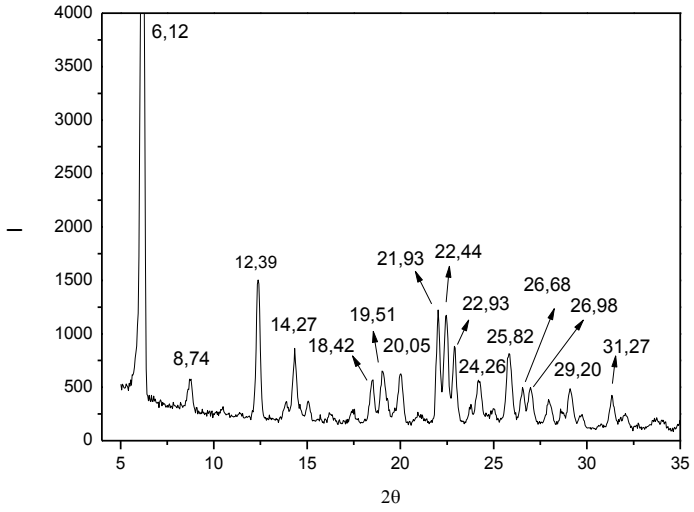

Figure S8. X-ray Powder Diffraction (PXRD) of **1.**

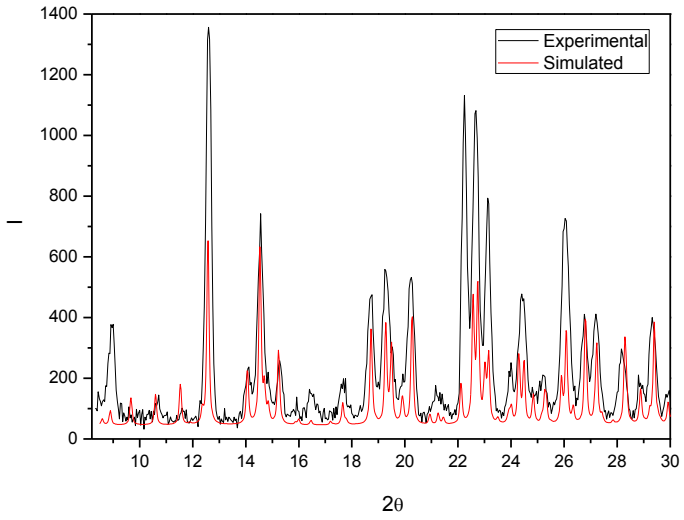

Figure S9 PXRD superimposed spectra of **1** of the spectrum calculated from single crystal diffraction using MERCURY software (red) and the PXRD experimentally obtained from the synthesis (black).

7) Crystal Data and Structural Refinement and selected distances and angles

An initial data collection revealed that the crystal contained a supercell. The second data collection involved two complete datasets, one at a collection tome of 1 s, the second at a collection time of 5 s. Both datasets were integrated together, and the full first dataset was treated as a fast scan in sadabs. This was done so that any overloaded reflections corresponding to the smaller cell could be scaled in. A solution was obtained in four space groups: *P*4/*ncc*, *P*4*cc*, $P42_12$, and $P\text{-}42_1c$. The initial R1 values were as follows:

R1	Rweak	Alpha	Orientation	Space group	Flack_x
0.315	0.002	0.067	as input	*P*4/*ncc*	
0.224	0.002	0.017	as input	*P*4*cc*	0.50
0.283	0.001	0.062	as input	$P42_12$	0.50
0.270	0.002	0.071	as input	$P\text{-}42_1c$	0.49

A complete refinement was conducted in *P*4/*ncc*, which showed that one of the two unique ligands was positionally disordered, while the other had some rotational disorder of the central aromatic ring. The positional disorder was modelled over two sites of complementary occupancy, with pairs of equivalent atoms constrained to have equal Uij values and SAME and SADI commands were used to ensure that the bond lengths and angles were equivalent for both orientations. The rotational disorder was modelled by generating remainder of the central -CH-C_6H_4-CH- from symmetry equivalent atoms and refining the entire unit with occupancy of 50%. SADI commands were used to constrain equivalent bonds to have the same length. Before modelling the BF_4 anions, a SQUEEZE analysis was performed. This showed the following:

```
loop_
   _platon_squeeze_void_nr
   _platon_squeeze_void_average_x
   _platon_squeeze_void_average_y
   _platon_squeeze_void_average_z
   _platon_squeeze_void_volume
   _platon_squeeze_void_count_electrons
   _platon_squeeze_void_content
    1  0.250  0.750  0.217      903      379 ' '
    2  0.250  0.750  0.250        7        0 ' '
    3  0.250  0.750  0.750        7        0 ' '
    4  0.750  0.250  0.781      903      379 ' '
    5  0.750  0.250  0.750        7        0 ' '
    6  0.750  0.250  0.250        7        0 ' '
_platon_squeeze_void_probe_radius          1.20
_platon_squeeze_details                    ?
```

As there were still anions needing to be modelled, no refinement was performed using SQUEEZE data, this was done for an estimate of residual electron density only. The above corresponds to 758 electrons per unit cell, or 63 electrons per Fe centre unaccounted for. One BF_4 contributes 42 electrons, so this leaves 21 electrons, or approximately 0.8 ethanol molecules unaccounted for. The bulk of the solvent used in the synthesis was ethanol, however, as there is a possibility that there may be small amounts of water present, these solvent molecules have not been included in the final molecular formula.

One BF_4 anion was modelled, and successive positions of the disordered BF_4 were added as more peaks of electron density appeared in the region. The BF_4 anions were refined with a common B-F bond length, which was refined as a free variable, and an F...F separation that was fixed at 1.633 times this value. Each BF_4 site was given a variable occupancy, with these constrained to sum to 0.75. Equivalent atoms were constrained to have equal Uij values.

As there were multiple potential space groups, one of which (*P*4*cc*) had a significantly lower initial *R*1 than the current model, the framework atoms were modelled for each of the other three potential solutions. The resulting *R*1 values, Flack parameters and BASF values are as follows:

*P*4*cc*	0.1502	0.52(10)	0.52085
$P4_12_12$	0.1482	0.52(13)	0.51576
P-42_1c	0.1513	0.51(12)	0.50817

In all cases, the R1 values are comparable to the current solution, and the Flack and BASF parameters indicate that the crystal is either centrosymmetric or a racemic twin. None of these lower symmetry space groups resulted in the ordering of the disordered ligands. As such, the space group *P*4/*ncc* was selected as the correct space group.

Table S1. Crystal data and structure refinement for compound 1.

Compound	(**1**)
CCDC	1825247
Chemical formula	$C_{72}\ H_{60}\ B_3\ F_{15}\ Fe_3\ N_{48}$
Formula mass	2082.66
Temperature (K)	100(2) K
Crystal system	Tetragonal
Space group	*P* 4/*n c c*
a/Å	19.9412(9)
b/Å	19.9412(9)
c/Å	24.1342(15)
α/◦	90
β/◦	90
γ/◦	90
V(Å^3)	9597.0(11)
Z	
Radiation type	Synchrotron
Density (calculated mg/m^3)	1.441
Absorption coefficient (mm^{-1})	0.683
F(000)	4224
Crystal size (mm^3)	0.130 x 0.120 x 0.080
Goodness of fit on F^2	2.717
*R*1, *wR*2 [$I>2\sigma(I)$]	0.1301, 0.4997
*R*1, *wR*2 (all data)	0.1508, 0.0576

Table S2. Selected bond lengths [Å] for compound **1**.

Fe(1)	
Fe(1)-N(1) 2.164(3)	Fe(1)-F(3) 1.943(6)
Fe(1)-F(3) 2.117(6)	Feav-X 2.119
Fe(2)	
Fe(2)-N(7) 2.166(3)	Fe(2)-F(1) 2.092(6)
Fe(2)-F(2) 1.927(6)	Feav-X 2.113
Fe(3)	
Fe(3)-N(9) 2.260(3)	Fe(3)-F(2) 2.035(5)
Fe(3)-F(3) 1.953(6)	Feav-X 2.171

Table S3. Selected angles [°] for compound **1**.

Fe(1)-F(1)-Fe(2)	180
Fe(2)-F(2)-Fe(3)	180
Fe(3)-F(3)-Fe(1)	180
F(1)-Fe(1)-F(3)	180
N(1)-Fe(1)-N(1)	167.40
N(1)-Fe(1)-N(1)	89.31
F(1)-Fe(1)-N(1)	96.30
F(3)-Fe(1)-N(1)	83.70

Table S4. Principal interactions [Å] for compound **1**

π···π contacts (C···C)	
C3_1-C6_1 3.337	C4_1-C5_1 3.392
C3_1-C(14) 3.214	
Lone pair π interaction	
N(11)-N(8) 3.078	
Hydrogen bonds	
F6_4-H8_1 2.559	F7_4-H(14) 2.327
F6_4-C8_1 3.363	F7_4-C(14) 3.258

8) Principal molecular interactions for compound 1. The distances are in concordance with the values founded in the literature[1]

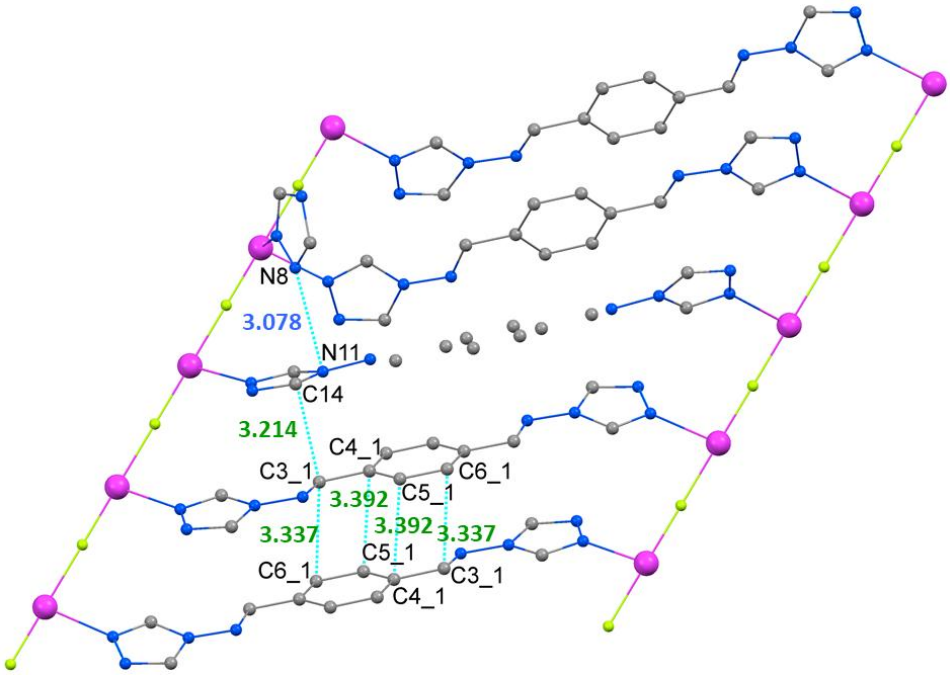

Figure S10 . This Figure shows the principals π···π and lone pair π interactions between the rings of the PM-tria ligand.

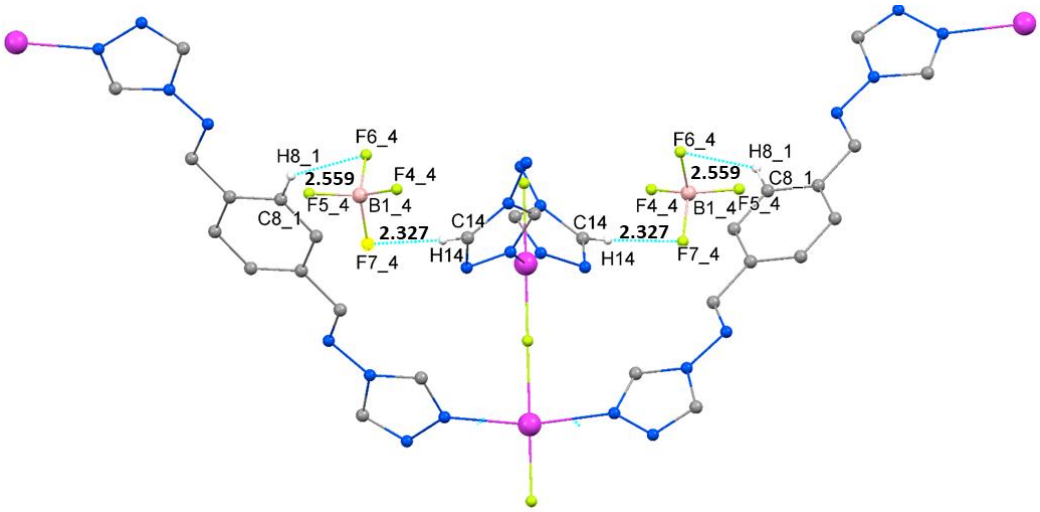

Figure S11. Representation of the weak interactions of the tetrafluoroborate counterions with the **PM-Tria** ligands

9) Illustration of the unusual rotation of the central metal equatorial coordination plane along *c* axis.

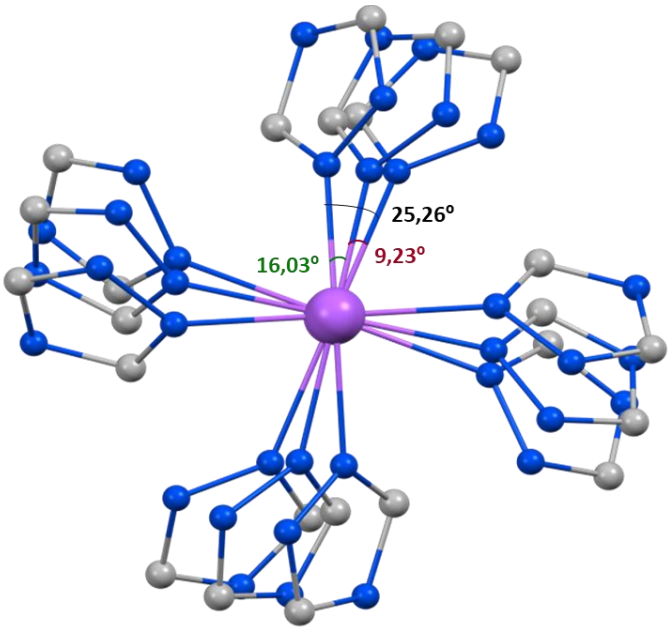

Figure S12. Illustration of the rotation of compound **1** along *c* crystallographic direction

10) BET Analysis

To evaluate the pore volume and surface area of this framework, the gas sorption isotherm was measured via BET studies. This representation (Fig. S13) shows the amount of gas adsorbed as a function of the relative pressure at constant temperature. The sorption of nitrogen revealed a type II isotherm, which is found in mesoporous and non-porous compounds. The pore diameter found was 13.6 nm which is characteristic of mesoporous materials. However a low surface area, 6.7 $m^2\ g^{-1}$ was observed, due to the hindrance of the pores by the ligands and/or the counter ions. Therefore, there is almost no N_2 adsorption on the surface of the MOF.

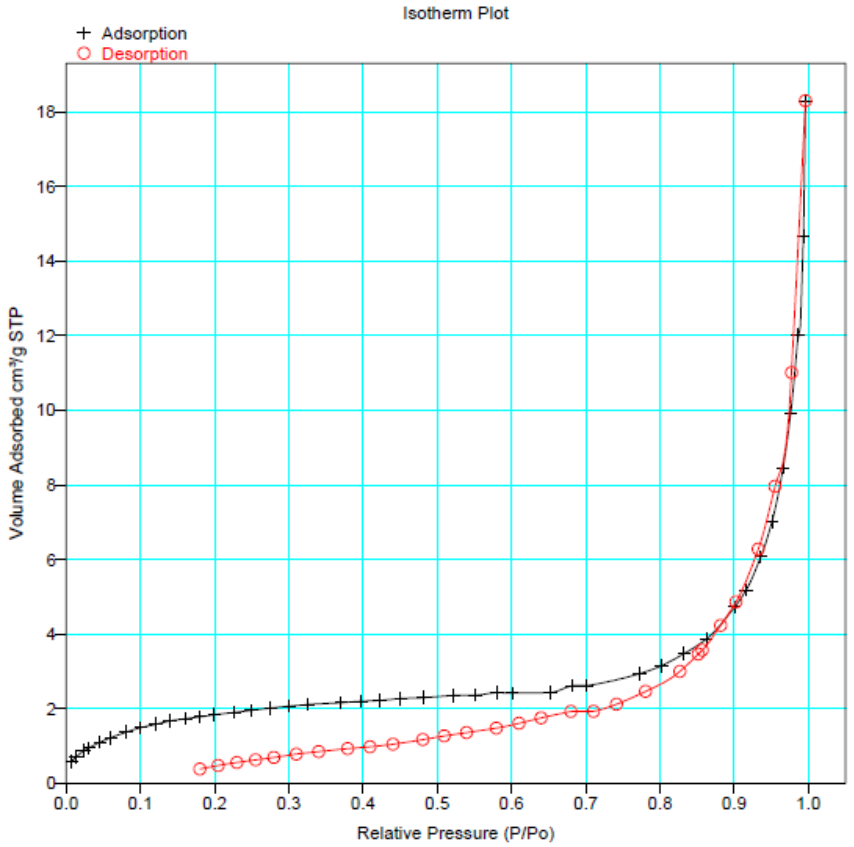

Figure S13. Nitrogen gas sorption isotherm at 78 K for compound **1**(filled circles, sorption; open circles desorption). P/P0 is the ratio of gas pressure (P) to saturation pressure (P0), with P0 being 716 torr.

11) Picture of the original mosaic found in the Alhambra Palace

Fig. S14. Islamic Mosaic

12) Magnetic behaviour

The analytical expression for an infinite chain of classical spins, as derived by Fisher from the exchange Hamiltonian:

$$H = -J \sum_{i=1}^{n-1} S_i \times S_{i+1}$$

and then, incorporating a paramagnetic contribution, $\chi_P = C_P/T$

$$\chi = \frac{Ng^2\beta^2 S(S+1)}{3kT} \frac{1+u}{1-u} + \chi_P$$

with

$$u = coth\left[\frac{JS(S+1)}{kT}\right] - \left[\frac{kT}{JS(S+1)}\right]$$

This model satisfactorily reproduces the the data in all the temperature range, with parameters S = 2, g = 2.12, J = –16 cm^{-1} and C_P = 0.03cm^3 K mol^{-1}

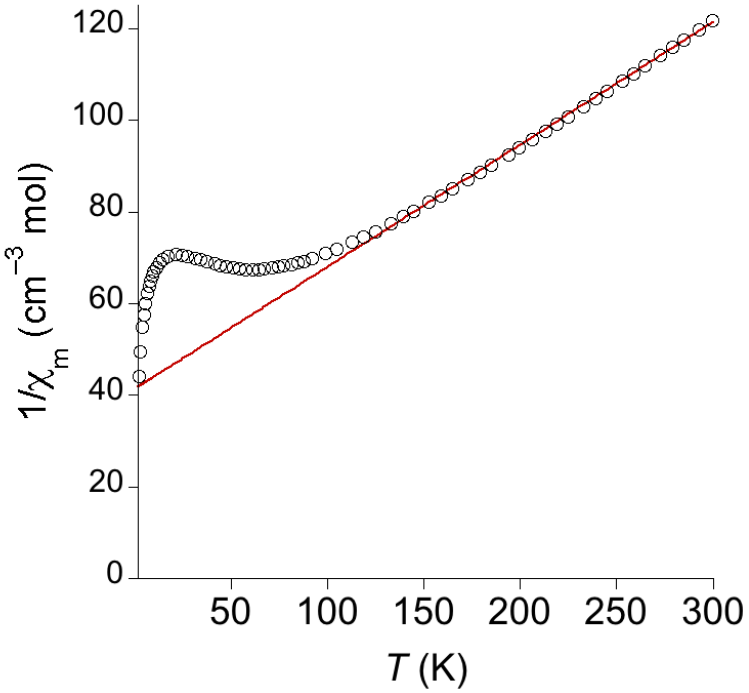

Fig. S15. High temperature regime fitted to a Curie-Weiss law with parameters C = 3.85 cm^3 K mol^{-1}, g = 2.24 and θ = –10.6 K.

13) Notes and references.

1. J. Mooibroek, P. Gamez and J. Reedijk, *CrystEngComm*, 2008, **10**, 1501–1515